THE JOURNAL OF PHYSICAL CHEMISTRY B

Article

pubs.acs.org/JPCB

Differential Binding Models for Isothermal Titration Calorimetry: Moving beyond the Wiseman Isotherm

Isaac Herrera and Mitchell A. Winnik*

Department of Chemistry, University of Toronto, 80 St. George Street, Toronto ON Canada M5S 3H6

Supporting Information

ABSTRACT: We present a set of model-independent differential equations to analyze isothermal titration calorimetry (ITC) experiments. In contrast with previous approaches that begin with specific assumptions about the number of binding sites and the interactions among them (e.g., sequential, independent, cooperative), our derivation makes more general assumptions, such that a receptor with multiple sites for one type of ligand species (homotropic binding) can be studied with the same analytical expression. Our approach is based on the binding polynomial formalism, and the resulting analytical expressions can be extended to account for any number of binding sites and any type of binding interaction among them. We refer to the set of model-independent differential equations to study ITC experiments as a differential binding model (DBM). To demonstrate the flexibility of our DBM, we present the analytical expressions to study receptors with one or two binding sites. The DBM for a receptor with one site is equivalent to the Wiseman isotherm but with a more intuitive representation that depends on the binding polynomial and the dimensionless parameter $c = K{\cdot}M_T$, where K is the binding constant and M_T the total receptor concentration. In addition, we show how to constrain the general DBM for a receptor with two sites to represent sequential, independent, or cooperative binding interactions between the sites. We use the sequential binding model to study the binding interaction between Gd(III) and citrate anions. In addition, we simulate calorimetry titrations of receptors with positive, negative, and noncooperative interactions between the two binding sites. Finally, we derive a DBM for titrations of receptors with n-independent binding sites.

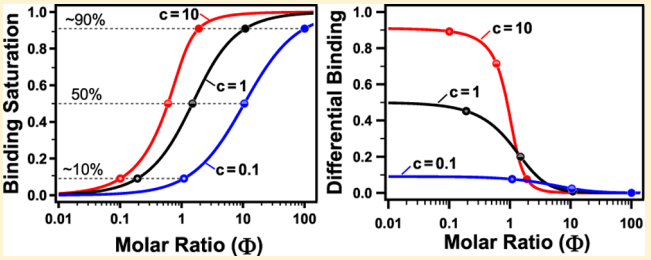

1. INTRODUCTION

Isothermal titration calorimetry (ITC) is an analytical technique to measure the heat of reaction from a binding process between two or more species in solution.[1,2] Similar to other titrimetric methods, the experiment is carried out by injecting a small volume of titrant into an analyte solution while a physical property of the system "signals" the binding event. In ITC, the signal measured at each injection step is proportional to the heat of reaction, a thermodynamic property. Therefore, ITC allows for the direct determination of the enthalpy (ΔH), the free energy (ΔG), and the entropy (ΔS) of the binding process, in addition to the stoichiometry (n) and the binding constant (K), giving a complete thermodynamic and quantitative characterization of the system. There are several reviews and reports about the characterization of receptor–ligand interactions using ITC, most of which are aimed at the characterization of biologically relevant receptors such as proteins,[3] polysaccharides,[4] polynucleotides,[5] or amphiphilic[6] species with their respective ligand counterparts. In addition, the major developments in ITC are reviewed on a yearly basis,[7−9] which points to the growth of the field during the past decade.

A crucial step in ITC is to analyze the binding data with a mathematical model that describes (i) the binding mechanism and (ii) the relation between the heat of reaction and the amount of titrant added. Commonly, the analysis of ITC experiments is carried out using the models embedded in the analysis software of the calorimeter. These built-in models can be applied to simple binding systems, but it is challenging to apply them to receptors with multiple binding sites.[10] There are some alternatives to analyze ITC experiments in the form of commercial software,[11] free software,[12−16] or mathematical models.[17−20] However, the binding models in these reports were constrained to represent receptors with a finite number of binding sites and specific binding interactions among the sites.

For this purpose, we derive a general set of differential equations to analyze ITC experiments which can be applied to receptors with multiple binding sites and different binding interactions among the sites. The differential equations have the form df/dx, where the term f is a variable related to the binding species in solution and the term x is an independent variable related to the progress of the titration experiment. We refer to this type of differential equations to study ITC experiments as differential binding models (DBMs).

The Wiseman isotherm (WI)[1] is the most well-known DBM, and it has been extensively applied to ligand-into-receptor

Received: November 30, 2012
Revised: April 24, 2013
Published: July 10, 2013

titrations of receptors with either *one* binding site ($n = 1$) or *n*-equivalent binding sites. The explicit expression of the WI model is given by

$$\frac{d[MX]}{dX_T} = \frac{1}{2} + \frac{1 - \Phi - 1/c}{2((1 + \Phi + 1/c)^2 - 4\Phi)^{1/2}} \quad (1)$$

where Φ is the degree of titration,[21] proportional to the ratio between the total concentration of ligand (X_T) and receptor (M_T) in the titration cell (i.e., mole ratio)

$$\Phi = \frac{X_T}{M_T} \quad (2)$$

and c is a dimensionless binding parameter, proportional to the product of the binding constant (K) and the total concentration of receptor species in the cell M_T, or also expressed as the ratio between M_T and the dissociation constant (K_d)

$$c = K \cdot M_T = M_T/K_d \quad (3)$$

The parameter c is important in the analysis of ITC experiments because it affects the shape of titration curves,[22,23] the mole equivalents of titrant required to saturate the binding sites in the receptor,[24] and the accuracy of the fitted binding parameters (e.g., n, K, ΔH).[25−28] However, dimensionless parameters similar to c for receptors with multiple binding sites have not been studied.

Some DBMs for receptors with two binding sites ($n = 2$) have been described in the literature.[20,29,30] For example, Indyk and Fisher[29] derived a differential expression to study a receptor with two independent sites. More recently, Poon derived DBMs for receptors with either independent or cooperative binding sites[20] by implicitly differentiating the mass-balance equation for the titration experiment. Although the derivation procedure used by Poon[20] is more efficient than that of Indyk and Fisher,[29] one needs to select the number of binding sites in the receptor and the type of binding interaction among the binding sites before the derivation of the model begins. Thus, analyzing more than one hypothetical binding model may be a time-consuming task.

In contrast with previous studies, we begin our derivation with a more general assumption based on the binding polynomial (P_M) of a homotropic binding system, which describes the distribution of the receptor-containing binding species in solution.[31,32] This powerful mathematical formalism has been widely utilized to study binding equilibrium reactions[33−36] as well as some titration calorimetry studies.[37−41] By implicitly differentiating a mass-balance equation expressed in terms of the binding polynomial, we obtain a general set of differential equations where the interactions among the binding sites are unconstrained.

To demonstrate the flexibility of our DBM, we simulate titration curves of receptors with *one* ($n = 1$) or *two* ($n = 2$) binding sites. For the theoretical evaluation, we use dimensionless variables proportional to the concentration of free ligand [X] and the binding constant of the fully saturated state. In the case of a receptor with $n = 1$, the dimensionless variable is $K[X]$, where K is the binding constant of the 1:1 receptor−ligand complex, while the variable $\beta_2^{1/2}[X]$ is used in the case of a receptor with $n = 2$, where $\beta_2^{1/2}$ represents the square root of the cumulative binding constant for the 1:2 complex. We can further constrain the DBM of a receptor with $n = 2$ to represent specific binding interactions between the two binding sites such as sequential, independent, or cooperative binding interactions. In the case of the cooperative binding model, we simulate titration calorimetry curves of receptors with positive (ρ^+), negative (ρ^-), and noncooperative interactions (ρ^0). Experimentally, we use the DBM with $n = 2$ to analyze the calorimetry titration of gadolinium with sodium citrate where the DBM is evaluated as a function of the total volume of titrant injected (V). Finally, we derive an alternative expression to study receptors with *n*-independent binding sites which explicitly shows the independent nature of each binding site. The DBMs derived in this Article contain dimensionless parameters similar to c (eq 3) that can be used to optimize the signal for the titration calorimetry experiment.

2. THEORETICAL BASIS

2.1. Binding Polynomial and Binding Potentials for a Homotropic Binding System. The concept of a binding polynomial was introduced by Wyman[31,32] more than a half-century ago, and its properties have been widely utilized to study binding equilibrium reactions between receptor and ligand species.[33−36] The theoretical formalism to analyze titration calorimetry experiments using the binding polynomial was originally presented by Gill et al.[37] and recently summarized by Freire et al.[40] In a separate study, Koper et al.[41] also utilized the properties of a binding polynomial to describe cooperativity effects in a macromolecular receptor as well as the micellization of various surfactants in solution. In this section, we provide a short description of the binding polynomial (P_M) for a homotropic system as well as the binding potentials obtained by partial differentiation of P_M with respect to ln[X], namely, the average ligand loading per receptor ($\bar{N}_X$) and the binding capacity (B_X).

The overall equilibrium reaction in terms of the cumulative binding constants (β_i) in a homotropic (one ligand) and homonuclear (no self-association) binding system is defined as

$$M + iX \rightleftarrows MX_i \qquad \beta_i = \frac{[MX_i]}{[M][X]^i} \quad (4)$$

The binding polynomial P_M represents the partition function for the binding species at equilibrium, normalized by the concentration of free receptor [M]. The expression for the binding polynomial in terms of the cumulative binding constants β_i is given by

$$P_M = \sum_{i=0}^{n} \beta_i [X]^i \quad (5)$$

By definition, the binding constant of the reference state is given by $\beta_0 = 1$ (i.e., $\beta_0 = [M]/[M]$). The mole fraction (α_i) of receptor species bound to i ligands is given by

$$\alpha_i = \frac{[MX_i]}{M_T} = \frac{\beta_i [X]^i}{P_M} \quad (6)$$

and it represents the normalized probability of finding the species MX_i at a given concentration of free ligand. In addition, the sum of all the mole fractions α_i for the receptor containing species is 1 (i.e., $\sum \alpha_i = 1$). In this representation of the binding system, the interactions among the binding sites are not constrained to a specific model. Hence, the binding polynomial formalism is sometimes referred to as model-independent. If a particular binding mechanism is required, the cumulative binding constants β_i can be expressed in terms of the

dx.doi.org/10.1021/jp311812a | J. Phys. Chem. B 2013, 117, 8659−8672

appropriate binding constants for independent, sequential, or cooperative binding models.[40]

The binding potentials $\bar{N}_X$ and B_X correspond to the state functions of a binding system at constant temperature and pressure obtained by partial differentiation of the free energy ($\Delta G^\circ = -RT \ln P_M$) with respect to the chemical potential ($\mu_X = \mu^\circ - RT \ln[X]$) of the free ligand.[31] In the derivation of the DBM, we use the expressions

$$\bar{N}_X = \left(\frac{\partial \ln P_M}{\partial \ln[X]}\right)_{T,P} = \frac{\sum_{i=0}^{n} i\beta_i[X]^i}{P_M} \tag{7}$$

$$B_X = \left(\frac{\partial^2 \ln P_M}{\partial(\ln[X])^2}\right)_{T,P} = \frac{\sum_{i=0}^{n} i^2\beta_i[X]^i}{P_M} - \left(\frac{\sum_{i=0}^{n} i\beta_i[X]^i}{P_M}\right)^2 \tag{8}$$

to represent both the binding and the statistical properties of the binding system. From a binding perspective, for example, $\bar{N}_X$ describes the binding saturation of a receptor, while the binding capacity B_X describes the ability of a receptor to bind more ligands as the chemical potential of the free ligand increases. From a statistical perspective, $\bar{N}_X$ represents the cumulative distribution function of the bound species, while B_X represents the probability density function.[42] In other words, $\bar{N}_X$ is proportional to the probability of finding a receptor bound to n ligands at a given chemical potential, while B_X is proportional to the variance in the number of ligands bound to the receptor.

2.2. Binding Models for Isothermal Titration Calorimetry (ITC). In a titration calorimetry experiment, the total heat of reaction (q) is proportional to the concentration of the species formed during the titration as given by

$$q = V_C \sum_{i=1}^{n} \Delta H_i[MX_i] \tag{9}$$

where V_C is the volume of the titration cell, n is the number of binding sites, ΔH_i is the molar heat of the reaction, and $[MX_i]$ is the molar concentration of the receptor (M) bound to i ligands (X) as shown in eq 4. For ITC, in particular, the signal collected at each injection point is proportional to the differential heat (Δq or dq), defined here as the change in the heat content of the cell after a small amount of titrant is added.

There are two major approaches to analyze the differential heat signal of an ITC experiment. In the first approach, the differential heat is evaluated as the finite difference between two consecutive injection points with an expression such as

$$\Delta q_k = V_C \cdot \sum_{i=1}^{n} \Delta H_i \left([MX_i]_k - \left(1 - \frac{\Delta V_k}{V_C}\right) \cdot [MX_i]_{k-1} \right) \tag{10}$$

where ΔV_k corresponds to the volume injected at step k, and the term $1 - \Delta V_k/V_C$ corrects for the dilution of the binding species. In the second approach, the differential heat (dq) is divided by the moles of titrant injected (dn_{inj}), and the resulting differential heat per mole (dH) can be expressed as a differential equation with the form

$$dH = \frac{1}{V_C} \cdot \frac{dq}{dX_T} = \sum_{i=1}^{n} \Delta H_i \frac{d[MX_i]}{dX_T} \tag{11}$$

where the moles of titrant injected dn_{inj} are commonly represented by the product of the cell volume and the change in the total concentration of ligand in the syringe ($dn_{inj} \approx V_C \cdot dX_T$). Reference 43 provides a detailed thermodynamic description of the differential heat that takes into account the differential volume.

Dimensional analysis of eq 11 shows that the terms dH, $V_C^{-1} \cdot dq/dX_T$, and ΔH_i all have units of heat per mole (e.g., kJ·mol^{-1} or kcal·mol^{-1}). In contrast, the differential $d[MX_i]/dX_T$ (eq 11) is dimensionless and its shape defines the titration calorimetry curve.[44] Therefore, finding mathematical formulas for the term $d[MX_i]/dX_T$ that properly describes the binding interaction between receptor and ligand species as well as the binding interactions among the binding sites is a crucial step in the analysis of ITC experiments.

2.3. Derivation of Differential Binding Models (DBMs) for ITC. The mass balance equations for M_T and X_T can be expressed in terms of P_M and $\bar{N}_X$ as given by

$$M_T = [M] \cdot P_M \tag{12a}$$

$$X_T = [X] + M_T \bar{N}_X \tag{12b}$$

where the term $M_T\bar{N}_X$ accounts for the concentration of ligand bound to the receptor. As previously shown by Poon,[20] expressions with the form $d[MX]/dX_T$ or $d[X]/dX_T$ can be derived by implicit differentiation of the explicit solution to the mass-balance equations (eq 12b) with respect to X_T. Using a similar methodology, we derive DBMs by implicit differentiation of the mass balance equation with respect to the degree of titration (Φ). To obtain a dimensionless representation of the mass balance expression, we divide eq 12b by M_T

$$\Phi = \frac{[X]}{M_T} + \bar{N}_X \tag{13}$$

In addition, we assume that M_T remains constant during the titration (i.e., no dilution) to simplify the derivation and theoretical evaluation to a single independent variable Φ.

The main contribution of this article is the general set of differentials (eqs 14a−14c) to study receptor species with n-binding sites. The general DBM consists of three differential equations proportional to (i) the concentration of free ligand ($M_T^{-1} \cdot d[X]/d\Phi$), (ii) the mole fractions of the receptor species bound to i ligands ($d\alpha_i/d\Phi$), and (iii) the average ligand bound per receptor ($d\bar{N}_X/d\Phi$), as given by

$$\left(\frac{1}{M_T}\right) \cdot \frac{d[X]}{d\Phi} = \frac{[X]}{[X] + M_T B_X} \tag{14a}$$

$$\frac{d\alpha_i}{d\Phi} = \frac{M_T \alpha_i (i - \bar{N}_X)}{[X] + M_T B_X} \tag{14b}$$

$$\frac{d\bar{N}_X}{d\Phi} = \frac{M_T B_X}{[X] + M_T B_X} \tag{14c}$$

The first step in our derivation is to obtain the differential $M_T^{-1} \cdot d[X]/d\Phi$ by implicitly differentiating the dimensionless mass balance equation (eq 13). Then, the differentials $d\alpha_i/d\Phi$ and $d\bar{N}_X/d\Phi$ are obtained using the chain rule (e.g., $d\alpha_i/d\Phi = (d\alpha_i/d[X]) \cdot (d[X]/d\Phi)$). The step-by-step derivation of eqs 14a−14c is shown in the Supporting Information (eqs S1−S31).

dx.doi.org/10.1021/jp311812a | J. Phys. Chem. B 2013, 117, 8659−8672

We can use eqs 14a−14c to evaluate the titration of a receptor with any number of binding sites, since the binding polynomial P_M (eq 5) and the terms α_i, $\bar{N}_X$, and B_X (eqs 6−8) derived from P_M contain the parameter n. Hence, to include an additional binding site in the model, we extend the summation terms in eqs 5−8 from n to $n + 1$. More importantly, the cumulative binding constants β_i can be expressed in terms of the stepwise (K_i), independent (k_i), or cooperative (κ_i) binding parameters.[31,40] Thus, the general DBMs in eqs 14a−14c can be easily adapted to represent a receptor with any number of binding sites and any type of binding interaction.

Expressions that resemble eq 14a have been used to study binding equilibrium reactions.[45−47] For example, the explicit solution for $M_T^{-1}\cdot d[X]/d\Phi$ in terms of the cumulative binding constants (β_i) is equivalent to the expression derived by Zhu et al. for the differential $d[X]/dX_T$.[45] The term $d[X]/dX_T$ was used to analyze protein−ligand titrations by mass spectrometry, where the hydrogen atoms of the amide linkages were exchanged by deuterium atoms (PLIMSTEX). In our DBM, we use the average ligand binding $\bar{N}_X$ and the binding capacity B_X in the explicit solution of eqs 14a−14c to simplify the notation.

To evaluate the differential heat per mole dH, we can use the differential $d\alpha_i/d\Phi$ (eq 14b) and its corresponding cumulative enthalpy of binding ΔH_i as given by

$$dH = \sum_{i=1}^{n} \Delta H_i \cdot \frac{d\alpha_i}{d\Phi} \tag{15}$$

which is equivalent to eq 11 (see the Supporting Information, eqs S23−S25). Similar to the cumulative binding constant β_i, the cumulative enthalpy of binding ΔH_i in eq 15 can be expressed in terms of the stepwise (ΔH_i^{i-1}), independent (Δh_i), or cooperative ($\Delta \eta_i$) enthalpies of binding to represent specific binding interactions among the binding sites.[40] Furthermore, eq 15 can be extended to account for the heat of dilution of the free ligand (Δh_{dil}), as given by

$$dH = \sum_{i=1}^{n} \Delta H_i \frac{d\alpha_i}{d\Phi} + \left(\frac{\Delta h_{dil}}{M_T}\right) \cdot \frac{d[X]}{d\Phi} \tag{16}$$

3. EXPERIMENTAL SECTION

3.1. Materials. Gadolinium(III) chloride hexahydrate (99.99%), disodium hydrogen citrate sesquihydrate (>99.9%), 2-(*N*-morpholino)ethanesulfonic acid hydrate (MES, >99.9%), sodium hydroxide (99.99% trace metal basis), and hydrochloric acid (TraceSELECT) were purchased from Sigma-Aldrich and used as received. The gadolinium and citrate salts were stored in a desiccator.

Gd(III) cations and citrate anions were chosen as binding species because they form both 1:1 and 1:2 receptor−ligand complexes.[48] A stock solution of $GdCl_3$ (50 mM) was prepared from the pure salt and acidified to pH 2.0 with concentrated HCl. Similarly, stock solutions of MES (250 mM) and sodium citrate (100 mM) were prepared from the pure salts and adjusted to pH 5.5 with NaOH (1.0 M) and HCl (1.0 M). All of the stock solutions were prepared using deionized water (Millipore 18 MΩ-cm). Buffered solutions of $GdCl_3$ (0.5 mM) and sodium citrate (10 mM) in MES buffer (100 mM) were prepared by diluting the stock solutions to the required concentration. The pH of the titrant and analyte solutions were measured, and their values were adjusted to pH 5.5, when necessary.

3.2. Isothermal Titration Calorimetry (ITC). The titration calorimetry experiments were performed using a VP-ITC calorimeter from MicroCal/GE Healthcare (Piscataway, NJ, USA). Prior to each titration, the solutions of titrant (sodium citrate) and analyte ($GdCl_3$) were sonicated and/or degassed for 15 min using the unit provided with the calorimeter. In addition, the titration cell was rinsed first with a dilute soap solution (5% CONTRAD 70, 2 mL), then with D.I. water (ca. 20 mL), and finally with a small volume of analyte solution (ca. 0.5 mL). For each titration experiment, the titration cell (V_C = 1.4037 mL) was filled with the dilute $GdCl_3$ solution in MES buffer, and the syringe (300 μL) was filled with the dilute sodium citrate solution in the same buffer. The titrations were performed by injecting 1.0 μL of titrant for the first injection point and 5.0 μL for the following injection points with a 300 s delay between injections. During the experiment, the titration mixture was stirred at 400 rpm and its temperature was dynamically adjusted by the instrument to 25.0 ± 0.1 °C, where the initial reference power was set to 41.84 μW (ca. 10 $\mu cal \cdot s^{-1}$). The calorimetry titration of gadolinium with citrate ligand was performed in triplicate.

3.3. Data Analysis. The differential power (dP) vs time raw data, commonly referred to as thermograms, were analyzed using Origin 7.0. The software automatically generates a baseline for the raw data, and each peak is integrated to give the differential heat (dq) as a function of the differential volume injected (dV). The baseline contains sharp features that contribute to the noise of the titration curve which may be removed using the smoothing filters in Origin 7.0[49] or using the NITPIC[50] software package. We removed these sharp features by applying 3−4 cycles of the Savitzky−Golay smoothing filter, and the thermogram was integrated using the smoothed baseline.

The differential heat per mole titration curves were analyzed using IGOR Pro (WaveMetrics Inc., Lake Oswego, OR, USA). The columns labeled as "DH" and "INVJ" in Origin 7.0, which correspond to the differential heat and the differential volume injected, respectively, were used to calculate the differential heat per mole (dH) and the total volume injected (V).

To account for the dilution of the binding species, the total concentration of ligand X_T, total concentration of receptor M_T, and the degree of titration Φ were calculated with the expressions

$$X_T = X_S \cdot (1 - \exp(-V/V_C)) \tag{17a}$$

$$M_T = M_0 \cdot \exp(-V/V_C) \tag{17b}$$

$$\Phi = X_S \cdot (\exp(V/V_C) - 1)/M_0 \tag{17c}$$

where X_S represent the concentration of ligand in the syringe and M_0 is the initial concentration of receptor in the titration cell. Expressions similar to eqs 17a−17c have been used to calculate the stepwise dilution of the binding species in a calorimeter with an overfill-type cell.[51]

The calorimetry titration curves (dH vs V) were averaged, and the standard deviation (σ_k) for each injection point k was calculated. The averaged $d\bar{H}_k$ values were fitted with a DBM that accounts for the appropriate number of binding sites in the receptor (n), enthalpies of binding, and binding constants for a specific binding interaction. We also include a stoichiometry coefficient (N) to account for small experimental errors in the

dx.doi.org/10.1021/jp311812a | J. Phys. Chem. B 2013, 117, 8659−8672

total concentration of receptor ($M_T^* = N{\cdot}M_T$) and an enthalpy of dilution (Δh_{dil}) to account for the heat exchanged by the injection of free ligand. We use the parameter n (lower case) to expand the summation terms in the binding polynomial and in the binding potentials (eqs 5−8), and this integer value is held constant during the analysis.

Experimentally, we follow three steps to analyze the titration curves of dH vs V. First, we use the Jenkins−Traub algorithm[52] to calculate the concentration of free ligand [X]. This algorithm finds the root of the explicit solution of the mass-balance polynomial

$$f([X]) = X_T - [X] - M_T\bar{N}_X = 0 \tag{17d}$$

using the dilution-adjusted concentration of the binding species (eqs 17a−17c) and the cumulative binding constants for each binding site. Second, we evaluate the DBM in eq 16 using the concentration of free ligand [X]. Finally, we determine the fitting parameters for the titration by minimizing the reduced chi-square value[53] (χ_ν^2) using the expression

$$\chi_\nu^2 = \frac{1}{\nu}\sum_k \left(\frac{d\bar{H}_k - f(V_k)}{\sigma_k}\right)^2 \tag{18}$$

where ν is the number of degrees of freedom obtained from the difference between the number of data points and the number of fitting parameters, $d\bar{H}_k$ is the averaged differential heat, $f(V_k)$ is the expression for dH in terms of the DBM (eq 16), and σ_k is the standard deviation at point k. The fitting routine uses a weighted nonlinear least-squares Levenberg−Marquardt method[54] and generates a set of fitting parameters, their respective uncertainty values, and a correlation matrix to evaluate the interdependence among the fitting parameters.

4. DBM FOR A RECEPTOR WITH *ONE* BINDING SITE

The differential binding model for a ligand-into-receptor titration of a receptor with *one* binding site ($n = 1$) is obtained by substituting the expressions for the binding polynomial P_M, the mole fractions α_i, and the binding potentials $\bar{N}_X$ and B_X into the general DBM (eqs 14a−14c). First, the expressions for the terms P_M, $\bar{N}_X$, and B_X when $n = 1$ are given by

$$P_M = 1 + K[X] \tag{19a}$$

$$\bar{N}_X = \frac{K[X]}{P_M} \tag{19b}$$

$$B_X = \frac{K[X]}{P_M^2} \tag{19c}$$

where K is the binding constant for the bound receptor MX (i.e., $K = \beta_1$). The mole fractions (eq 6) of the free (α_0) and bound (α_1) receptor species are equivalent to P_M^{-1} and $\bar{N}_X$, respectively.

Second, we substitute eqs 19a−19c into the general DBM (eqs 14a−14c). The system of differential equations that allows us to evaluate the differential change in the concentration of free ligand, the mole fraction of the receptor species, and the average ligand binding saturation is given by

$$\left(\frac{1}{M_T}\right)\cdot\frac{d[X]}{d\Phi} = \frac{P_M^2}{c + P_M^2} \tag{20a}$$

$$\frac{d\alpha_1}{d\Phi} = \frac{d\bar{N}_X}{d\Phi} = \frac{c}{c + P_M^2} \tag{20b}$$

where c is the dimensionless term defined in eq 3. When $n = 1$, the differential $d\alpha_1/d\Phi$ is equivalent to $d\bar{N}_X/d\Phi$ because only one of the binding species contributes to the average ligand saturation. More importantly, the differential $d\alpha_1/d\Phi$ is equivalent to the Wiseman isotherm (eq 1) but with a much simpler form in terms of c and P_M.

Finally, we obtain an expression to evaluate dH for a receptor with $n = 1$ using the general form of the differential heat per mole dH (eq 15) and the explicit form of $d\alpha_1/d\Phi$ (eq 20b)

$$dH = \frac{\Delta H{\cdot}c}{c + P_M^2} \tag{21}$$

where we assume a negligible contribution to the differential heat per mole from the dilution of the free ligand. In the Supporting Information, we show an algebraic expression to evaluate the binding polynomial P_M in terms of Φ and c (eq S46), which in combination with eq 21 and the dilution expressions (eqs 17a−17c) can be applied to ITC experiments of receptors with one binding site.

4.1. Theoretical Evaluation of the Binding Potentials with *n* = 1. In Figure 1, we evaluate $\bar{N}_X$ and B_X using the dimensionless variable $K[X]$ to illustrate the properties of the binding potentials independently of the absolute value of the binding constant K. The binding potentials were evaluated in the range $10^{-3} \le K[X] \le 10^3$, which covers a binding saturation range from 0.01 to 99.9%. The plot of $\bar{N}_X$ with respect to $K[X]$ (Figure 1A) shows a binding saturation curve with a rectangular hyperbola shape where the receptor reaches 50% saturation ($\bar{N}_X = 0.5$) at $K[X] = 1$. In other words, the concentration of free ligand at half-saturation is inversely proportional to K, or directly proportional to the dissociation constant K_d ($[X]^{50\%} = 1/K = K_d$). In addition, the values of $\bar{N}_X$ at $K[X] = 1/10$ and $K[X] = 10$ correspond to 10 and 90% receptor saturation, respectively. The range of free ligand concentrations between the 10 and 90% saturation points corresponds to the minimum titration range for a binding experiment where the free ligand concentration can be directly measured during the titration (i.e., independent variable).

The semilogarithmic plots of the binding potentials with respect to $\log K[X]$ show the typical sigmoidal shape of a binding saturation curve $\bar{N}_X$ (Figure 1B) and the bell shape of a binding capacity curve B_X (Figure 1C). The semilogarithmic representations show the thermodynamic and probability properties of $\bar{N}_X$ and B_X. For example, the sigmoidal curve of $\bar{N}_X$ represents the average or most probable ligand saturation at a given chemical potential ($\mu_X = \mu^0 - \ln(10)RT{\cdot}\log[X]$) and has similar properties to a cumulative distribution function. Similarly, the bell shape of B_X, which has been used to describe the buffering capacity of acids and bases[21] and to examine the cooperativity of a receptor with n-binding sites,[36] is representative of a probability distribution function. In both semilogarithmic plots, the 10% saturation point corresponds to one log unit below the half-saturation point, while the concentration of free ligand at 90% saturation is one log unit above the half-saturation point. The exact values of the binding potentials at 10 and 90% are calculated with eqs 19a−19c using the values $K[X] = 1/10$ and $K[X] = 10$, respectively.

4.2. Theoretical Evaluation of $\bar{N}_X$ and $d\bar{N}_X/d\Phi$ in a Titration Experiment. In ITC experiments, the degree of titration (Φ) is commonly used as the abscissa to plot a

dx.doi.org/10.1021/jp311812a | J. Phys. Chem. B 2013, 117, 8659−8672

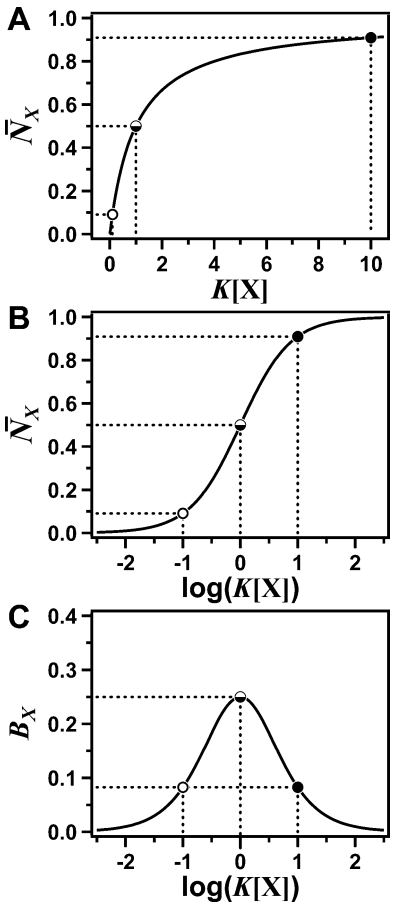

Figure 1. Linear and semilogarithmic plots of the average ligand saturation $\bar{N}_X$ and the binding capacity B_X for a receptor with $n = 1$ and a binding polynomial $P_M = 1 + K[X]$. The 10, 50, and 90% saturation points are indicated, respectively, by open (○), half-filled (◒), and filled circles (●). (A) $\bar{N}_X$ has a hyperbolic shape consistent with the saturation of the receptor at increasing concentrations of free ligand. (B) The binding potential $\bar{N}_X$, or binding isotherm, has a sigmoidal shape when plotted on a semilogarithmic axis. (C) The binding capacity B_X has a bell shape with a maximum value at half-saturation.

calorimetry titration curve. The term Φ can be expressed either as the ratio between the moles of ligand and the moles of receptor in the titration cell (eq 2) or as a dimensionless mass-balance equation (eq 13). For the theoretical analysis of a titration experiment, we evaluate the term Φ using the dimensionless variable $K[X]$

$$\Phi = \frac{K[X]}{1 + K[X]} + \frac{K[X]}{c} \tag{22}$$

where the first term corresponds to $\bar{N}_X$ (eq 19b) and c is the dimensionless binding constant for the titration (eq 3). Thus, the degree of titration Φ to saturate 90% of the receptor species in solution ($K[X] = 10$) can be calculated with the expression

$$\Phi_{90\%} = \frac{10}{11} + \frac{10}{c} \tag{23}$$

which is similar to the empirical expression obtained by Tellinghuisen to optimize the final degree of titration (Φ_f)[24]

$$\Phi_f = \frac{6.3}{c^{0.2}} + \frac{13}{c} \tag{24}$$

Additional expressions to evaluate the degree of titration Φ as a function of $\bar{N}_X$ and c are shown in the Supporting Information (eqs S39 and S40a–S40c).

In Figure 2, we simulate integral ($\bar{N}_X$) or differential ($d\bar{N}_X/d\Phi$) titration experiments by evaluating eqs 19b, 20b, and 22 in

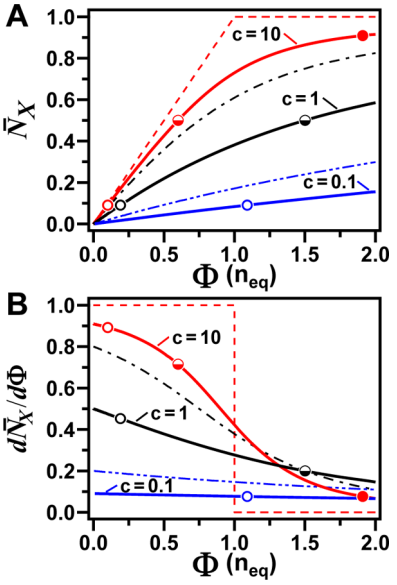

Figure 2. Titration representation of the average ligand binding $\bar{N}_X$ and the differential binding saturation $d\bar{N}_X/d\Phi$ for a receptor with one binding site ($n = 1$) and c values equal to 10, 1, and 0.1. The dashed lines were simulated with the values $c \to \infty$ (dashed line), $c = 4$ (dash-dotted line), and $c = 0.25$ (dash-double-dotted line) and represent the boundary values for titrations with high, medium, and low c values. The 10, 50, and 90% saturation points are labeled with open (○), half-filled (◒), and filled circles (●), respectively. (A) The plot of $\bar{N}_X$ vs Φ transitions from a trapezoidal shape at high c to a linear shape at low c when evaluated over the titration range from Φ = 0.0 to Φ = 2.0. (B) The plot of $d\bar{N}_X/d\Phi$ vs Φ shows an apparent loss of the sigmoidal shape for titrations with medium and low c values.

the range $10^{-3} \le K[X] \le 10^3$ and by plotting the terms $\bar{N}_X$ and $d\bar{N}_X/d\Phi$ with respect to Φ. We define three ranges for the parameter c by using the limiting value of the differential $d\bar{N}_X/d\Phi$ at the beginning of the titration (i.e., $K[X] = 0$)

$$\left.\frac{d\bar{N}_X}{d\Phi}\right|_{K[X]=0} = \frac{c}{1 + c} \tag{25}$$

which represents the initial slope of the titration curve of $\bar{N}_X$ vs Φ and is similar to the expression derived by Indyk and Fisher[29] for $d[MX]/dX_T$ (eq 1) when evaluated at $X_T = 0$. The three titration ranges are defined as follows: $c \ge 4$ is high and gives $d\bar{N}_X/d\Phi \ge 0.8$; c in the range $4 > c > 1/4$ is medium and gives differential binding curves in the range $0.8 > d\bar{N}_X/d\Phi > 0.2$; $c \le 1/4$ is low and gives values of $d\bar{N}_X/d\Phi \le 0.2$. The titration curves of $\bar{N}_X$ and $d\bar{N}_X/d\Phi$ with solid lines (Figure 2) were simulated with c values in each titration range (c = 10, 1, and 0.1 for high, medium, and low, respectively). In each titration curve, we indicate the points for 10, 50, and 90% average ligand saturation $\bar{N}_X$ using open, half-filled, and filled circles, respectively. The values of Φ and $d\bar{N}_X/d\Phi$ at 10, 50, and 90% average ligand saturation were calculated using eqs 22 and 20b, respectively. Titration curves with dashed lines were simulated with c values at the boundaries of each titration range

dx.doi.org/10.1021/jp311812a | J. Phys. Chem. B 2013, 117, 8659–8672

which correspond to $c \rightarrow \infty$ (dashed line), $c = 4$ (dash-dotted line), and $c = 1/4$ (dash-double-dotted line).

The relationship between the average ligand binding $\bar{N}_X$ with respect to the degree of titration Φ is shown in Figure 2A. Plots of $\bar{N}_X$ vs Φ are commonly used to represent thermometric[22] and UV−vis[23] titrations, where the bound species and its signal increases in relation to the total amount of ligand added. Titrations with a high c value begin with a trapezoidal shape in the limit of $c \rightarrow \infty$, which transitions into a rectangular hyperbola as the value decreases to $c = 4$. The titration experiment with $c = 10$ has a shape that resembles $\bar{N}_X$ in Figure 1A. Titration curves with a medium c value begin with a hyperbolic shape at $c = 4$ which transitions into a line shape as c decreases to 0.25. The titration simulated with $c = 1$ shows that the receptor reaches approximately 60% saturation after two mole equivalents of ligand are added. Finally, for titration curves with a low c value, the initial slope of the titration curve for $\bar{N}_X$ vs Φ is directly proportional to c. For example, the titration of a receptor with $c = 0.1$ reaches approximately 10% saturation after one mole equivalent of ligand is added. The hyperbolic shape for titrations with medium and low c values can be shown by increasing the end value for the degree of titration to $\Phi = 5$ and $\Phi = 25$, respectively (see the Supporting Information, Figure S2).

The plot of $d\bar{N}_X/d\Phi$ vs Φ in Figure 2B is a dimensionless representation of an ITC experiment for a receptor with one binding site.[26] The differential binding curves for titrations with a high c value begin with a shape that resembles a step function in the limit of $c \rightarrow \infty$ (dashed line) which then transitions into a sigmoidal shape as the value of c decreases to 4 (dash-dotted line). Titrations with medium c values begin with a nearly sigmoidal shape which then transitions into a decaying exponential shape as the value of c decreases to 0.25. Finally, titrations with a low c value have a nearly linear shape when evaluated with respect to Φ.

The differential $d\bar{N}_X/d\Phi$ represents the slope of the titration curve $\bar{N}_X$ vs Φ. For example, $\bar{N}_X$ increases linearly when $c \rightarrow \infty$ (Figure 2A, dashed line) for the titration points before the equivalence point (i.e., $\Phi < 1$) and remains constant for the titration points after the equivalence point (i.e., $\Phi > 1.0$). Therefore, the slope of the titration curve is given by $d\bar{N}_X/d\Phi \approx 1.0$ (i.e., linear) for $\Phi < 1$ and $d\bar{N}_X/d\Phi \approx 0$ (i.e., constant) for $\Phi > 1$ (Figure 2B, dashed line). The value of the differential $d\bar{N}_X/d\Phi$ is also related to the fraction of ligand bound for each addition of titrant.[27] For example, the percentage of ligand bound during the first injection of titrant is close to 90% when $c = 10$, 50% when $c = 1$, and only 10% when $c = 0.1$.

4.3. Semilogarithmic Evaluation of $\bar{N}_X$ and $d\bar{N}_X/d\Phi$ in a Titration Experiment. In this section, we use a semilogarithmic representation of $\bar{N}_X$ and $d\bar{N}_X/d\Phi$ for experiments with high, medium, and low c values ($c = 10$, 1, and 0.1, respectively). In addition, we evaluate $\bar{N}_X$ and $d\bar{N}_X/d\Phi$ with the boundary c values for each titration range, as given by $c \rightarrow \infty$ (dashed line), $c = 4$ (dash-dotted line), and $c = 0.25$ (dash-double-dotted line). The main benefit of using a semilogarithmic axis compared to a linear axis is that we show the full titration range from 10 to 90% for all the titration curves.

The plot of the average ligand saturation $\bar{N}_X$ with respect to $\log \Phi$ (Figure 3A) shows titration curves with an asymmetric sigmoidal shape for experiments with high and medium c values, which transitions into a symmetrical sigmoidal shape for experiments with low c values. The titration curve for an experiment with $c = 0.1$ has the same shape as the semilogarithmic plot of $\bar{N}_X$ vs $\log K[X]$ (Figure 1B). The similarity between these two curves indicates that most of the ligand added remains free in solution (i.e., $[X] \approx X_T$). The 50% saturation point for a titration with low c values is given by $-\log c$, or simply pc, where p is the mathematical operator for $-\log$. In addition, the titration range from 10 to 90% ligand saturation corresponds to $\log \Phi$ values equal to $pc - 1$ and $pc + 1$, respectively.

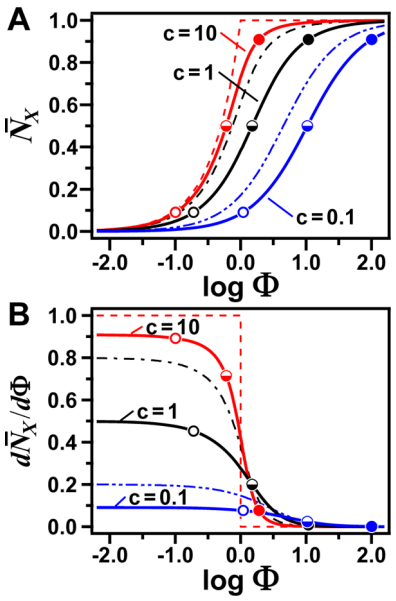

Figure 3. Semilogarithmic representation of the average ligand binding $\bar{N}_X$ and the differential binding saturation $d\bar{N}_X/d\Phi$ with respect to log Φ for receptors with one binding site ($n = 1$) and c values equal to 10, 1, and 0.1. The dashed lines were simulated with the values $c \rightarrow \infty$ (dashed line), $c = 4$ (dash-dotted line), and $c = 0.25$ (dash-double-dotted line) and represent the boundary values for each titration range. The 10, 50, and 90% saturation points are indicated, respectively, by open (○), half-filled (◒), and filled circles (●). (A) The semilogarithmic plot of $\bar{N}_X$ vs log Φ was evaluated from $\Phi = 10^{-2}$ to $\Phi = 10^{2}$. (B) The plot of $d\bar{N}_X/d\Phi$ vs log Φ shows that all the differential binding curves have a sigmoidal shape where the initial value depends on the value of c, as shown with eq 25.

Figure 3B shows the differential binding curves of $d\bar{N}_X/d\Phi$ with respect to log Φ for receptors with $n = 1$ and c values equal to 10, 1, and 0.1, where all the curves have a sigmoidal shape. Additional differential binding curves with other c values in each titration range also show a sigmoidal shape (see the Supporting Information, Figures S3 and S4). Semilogarithmic plots[41,47] as well as injection protocols where the volume injected at each injection step increases exponentially[55] have been used to show the full titration range of ITC experiments that involve surfactant species. More recently, Douglass et al.[56] also used a semilogarithmic plot to study the theoretical properties of the titration curve for a three-body binding model. There are two additional benefits for using a semilogarithmic axis to plot binding experiments. First, more experimental points in the range from $\Phi = 10^{-2}$ to $\Phi = 10^{-0.5}$ can be used to calculate the enthalpy of binding more accurately. Second, the end-point for the sigmoidal transition in the differential binding curve can be defined as the end-point for the titration. Thus, a titration with $c = 10$ (red line) has an end-point at $\Phi = 3.2$ (i.e., $\log \Phi \approx 0.5$). In comparison, the value calculated with eq 24 is $\Phi_f = 5.3$ (i.e., $\log \Phi_f \approx 0.72$).

dx.doi.org/10.1021/jp311812a | J. Phys. Chem. B 2013, 117, 8659−8672

Table 1. Mathematical Relation between the Binding Parameters in the General DBM for a Receptor with $n = 2$ (eqs 27a−27c) and the DBM for Receptors with Specific Binding Interactions between the Sites

	cumulative binding parameters				
	β_1	β_2	ΔH_1	ΔH_2	P_M
sequential sites	K_1	K_1K_2	ΔH_1^0	$\Delta H_1^0 + \Delta H_2^1$	$1 + K_1[X] + K_1K_2[X]^2$
independent sites	$k_{11} + k_{21}$	$k_{11}k_{21}$	$(\Delta h_1 \cdot k_{11} + \Delta h_2 \cdot k_{21})/(k_{11} + k_{21})$	$\Delta h_1 + \Delta h_2$	$(1 + k_{11}[X])(1 + k_{21}[X])$
equivalent sites	$2k$	k^2	Δh	$2\Delta h$	$(1 + k[X])^2$
cooperative sites	$2\kappa_1 k$	$\kappa_2 k^2$	$\Delta h + \Delta \eta_1$	$2\Delta h + \Delta \eta_2$	$1 + 2\kappa_1 k[X] + \kappa_2(k[X])^2$

5. DBM FOR A RECEPTOR WITH *TWO* BINDING SITES

The general DBM for a receptor with two binding sites is derived using the same procedure as previously shown for a receptor with $n = 1$. First, we define the general binding polynomial in terms of the cumulative binding constants, as given by

$$P_M = 1 + \beta_1[X] + \beta_2[X]^2 \tag{26}$$

where β_1 and β_2 correspond to the equilibrium reactions described in eq 4 for $i = 1$ and $i = 2$, respectively. Then, we evaluate the general form of the DBM (eqs 14a−14c) with the explicit expressions for the mole fractions α_1 and α_2 (eq 6) and the binding potentials $\bar{N}_X$ and B_X (eqs 7 and 8) with $n = 2$. The set of model-independent equations to evaluate the differential heat per mole dH of a receptor with two binding sites is given by

$$dH = \Delta H_1 \frac{d\alpha_1}{d\Phi} + \Delta H_2 \frac{d\alpha_2}{d\Phi} \tag{27a}$$

$$\frac{d\alpha_1}{d\Phi} = \frac{M_T\beta_1(1 - \beta_2[X]^2)}{P_M{}^2 + M_T(\beta_1 + 4\beta_2[X] + \beta_1\beta_2[X]^2)} \tag{27b}$$

$$\frac{d\alpha_2}{d\Phi} = \frac{M_T\beta_2[X](2 + \beta_1[X])}{P_M{}^2 + M_T(\beta_1 + 4\beta_2[X] + \beta_1\beta_2[X]^2)} \tag{27c}$$

The step-by-step derivation of eqs 27a−27c is shown in the Supporting Information (eqs S50−S59), where we also include the expressions for the differentials $M_T{}^{-1} \cdot d[X]/d\Phi$ and $d\alpha_0/d\Phi$. The overall change in the average number of ligands bound per receptor species $d\bar{N}_X/d\Phi$ for a receptor with two binding sites can be calculated using eqs 27b and 27c, as given by

$$\frac{d\bar{N}_X}{d\Phi} = \frac{d\alpha_1}{d\Phi} + 2 \cdot \frac{d\alpha_2}{d\Phi} \tag{28}$$

The general DBM for a receptor with two binding sites (eqs 27a−27c) can be modified to represent different binding interactions between the two sites. Table 1 shows the mathematical relation between the binding parameters in eqs 26 and 27a−27c and the binding parameters for receptors with specific binding interactions. For a detailed review of the relation between the cumulative binding constants and the binding constants for independent, equivalent, or cooperative binding sites, see ref 40. In addition, we include a step-by-step derivation of the DBMs for receptors with sequential, independent, or equivalent binding interactions in the Supporting Information (sections C.2−C.4).

5.1. Independent and Cooperative Binding Models. Cooperative interactions in receptors with two or more binding sites are observed if the affinity of a binding site changes due to the occupancy of other neighboring sites. The cooperative effect is positive if the affinity of a site increases when a neighboring site is bound. Conversely, the cooperative effect is negative if the affinity of the site decreases when the neighboring site is occupied. Finally, the interactions among the binding sites are referred to as independent or noncooperative if the affinity of the site remains the same regardless of the occupancy of the neighboring sites.

The binding model for a receptor with noncooperative binding interactions is equivalent to the model that describes a receptor with equivalent binding sites (Table 1), where k is the intrinsic binding constant for the independent binding site, and the cumulative binding constants in eqs 27b and 27c are given by $\beta_1 = 2k$ and $\beta_2 = k^2$. If the cumulative binding constants differ from the values expected due to the multiplicity of each binding state, then the receptor has cooperativity interactions.

As shown in Table 1, the binding polynomial for a receptor with two binding sites and cooperativity binding interactions is given by

$$P_M = 1 + 2\kappa_1 k[X] + \kappa_2 k^2[X]^2 \tag{29}$$

where the cooperativity coefficient (κ_i)[57] indicates the relative change in the binding affinity of the site with cooperative interactions in relation to an independent binding site. Thus, the condition for cooperativity in a receptor with two binding sites can be written in terms of the stepwise cooperativity parameter (ρ),[40] as given by

$$\rho = \frac{4\beta_2}{(\beta_1)^2} = \frac{4K_2}{K_1} = \frac{\kappa_2}{(\kappa_1)^2} \tag{30}$$

Positive cooperativity (ρ^+) is observed when $\rho > 1$ and $\kappa_2 > (\kappa_1)^2$, resulting in an increase in the stability of the doubly bound state (i.e., MX_2) with increasing binding saturation. Negative cooperativity (ρ^-) is observed when $\rho < 1$ and $\kappa_2 < (\kappa_1)^2$, resulting in a destabilization of the doubly bound state. Finally, noncooperativity (ρ^0) is observed when $\rho = 1$ and $\kappa_2 = (\kappa_1)^2 = 1$. This means that the binding saturation is only affected by the statistical factors for each bound state.

5.2. Theoretical Evaluation of the Binding Potentials with $n = 2$. Figure 4 shows the plots for the binding potentials $\bar{N}_X$ and B_X for a receptor with two binding sites. We evaluate the binding potentials $\bar{N}_X$ and B_X as a function of the dimensionless variables $\beta_2{}^{1/2}[X]$ and ρ, where $\beta_2{}^{1/2}$ is the square root of the second cumulative constant and ρ is the stepwise cooperativity parameter shown in eq 30. We simulate three possible cooperativity scenarios given by $\rho = 25$ for positive cooperativity (ρ^+), $\rho = 1$ for noncooperativity (ρ^0), and $\rho = 1/25$ for negative cooperativity (ρ^-). The linear plot of the average ligand saturation $\bar{N}_X$ (Figure 4A) was scaled by $\beta_2{}^{1/2}$, and the semilogarithmic plots of $\bar{N}_X$ and B_X (Figure 4B,C) were shifted by $\log \beta_2/2$ to show curves that are independent of the absolute value of β_2. In each plot, we label the points that correspond to 10, 50, and 90% binding saturation.

dx.doi.org/10.1021/jp311812a | J. Phys. Chem. B 2013, 117, 8659−8672

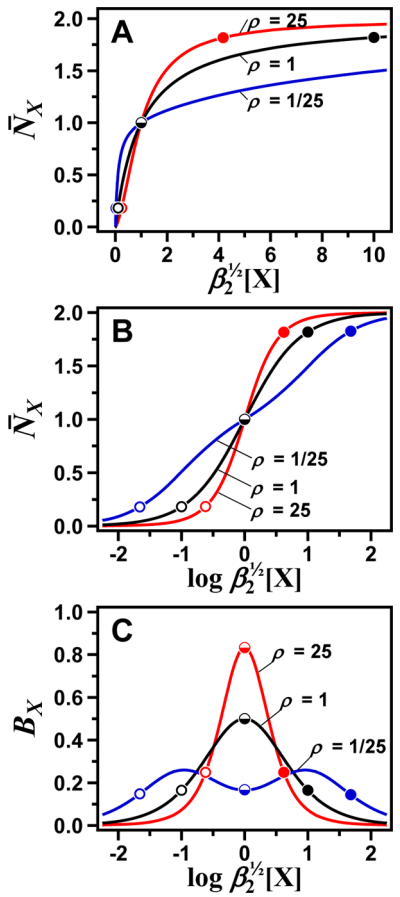

Figure 4. Effect of cooperativity parameters (ρ) on the binding potentials $\bar{N}_X$ and B_X for a receptor with *two* binding sites. The 10, 50, and 90% saturation points in the curves of $\bar{N}_X$ and B_X are indicated, respectively, by open (○), half-filled (◒), and filled circles (●). (A) The linear plot shows the binding saturation $\bar{N}_X$ versus the concentration of free ligand. The free ligand is scaled by $(\beta_2)^{1/2}$ so that the *x*-axis is independent of the absolute value of the binding constant. (B) The semilogarithmic plot of $\bar{N}_X$ shows the full titration range from 10 to 90% saturation in all three cooperative cases. (C) The semilogarithmic plots of B_X show bell-shaped curves. The plot of B_X for a receptor with negative cooperativity (ρ = 1/25) has two maxima at $\log \beta_2^{1/2}[X] = -1.0$ and 1.0.

In Figure 4A, the concentration of free ligand at half-saturation ($[X]^{50\%}$) is the same for all three curves of $\bar{N}_X$ (half-filled circles) regardless of the value of the cooperativity parameter ρ, where the concentration $[X]^{50\%}$ is equal to $\beta_2^{-1/2}$. Since the half-saturation point (i.e., $\bar{N}_X = 1$) is independent of the cooperativity parameter ρ, the term $\beta_2^{1/2}$ can be used to compare the overall binding strength of receptors with different cooperativity ρ values. On the other hand, the concentration of free ligand at 10 (open circles) and 90% saturation (filled circles) depends on both $\beta_2^{1/2}$ and ρ. For example, the concentration $[X]^{90\%}$ can be evaluated with the expression

$$[X]^{90\%} = \frac{1}{(\rho\cdot\beta_2)^{1/2}}\left(\frac{9}{2} + \left(\left(\frac{9}{2}\right)^2 + 10\rho\right)^{1/2}\right) \tag{31}$$

In the case of a receptor with independent binding sites (ρ = 1), the concentration $[X]^{90\%}$ is proportional to $10/(\beta_2)^{1/2}$. The ratio between $[X]^{90\%}$ and $[X]^{50\%}$ in a receptor with two independent sites is equivalent to the ratio obtained for a receptor with *one* binding site (i.e., $[X]^{90\%} = 10\cdot[X]^{50\%}$). The concentration $[X]^{90\%}$ decreases in receptors with positive cooperativity (e.g., $[X]^{90\%} \approx 4.2/\beta_2^{1/2}$ when ρ = 25), but $[X]^{90\%}$ increases in receptors with negative cooperativity (e.g., $[X]^{90\%} \approx 45/\beta_2^{1/2}$ when ρ = 25). Therefore, the concentration of free ligand at 90% receptor saturation is an indirect measure of the free energy required to reach the thermodynamic end-point of the titration. In other words, receptors with positive cooperativity interactions are more stable than receptors with negative cooperative interactions if both receptors have the same cumulative binding constant β_2.

Figure 4B shows the semilogarithmic plot of the average ligand saturation curves of $\bar{N}_X$. The binding isotherms have a sigmoidal shape that depends on the value of the stepwise cooperativity parameter ρ. Receptors with positive (ρ^+) and noncooperative (ρ^0) binding interactions between the two binding sites have only one inflection point situated at the half-saturation point ($\log \beta_2^{1/2}[X] = 0$). In contrast, the binding isotherm for a receptor with a negative cooperativity of ρ = 1/25 has two inflection points. Each inflection point is situated at nearly one log unit from the half-saturation point. In a semilogarithmic plot, we can also observe that the 10 and 90% saturation points in each binding isotherm, which define the titration range, are symmetric with respect to the half-saturation point. Thus, the titration range between 10 and 90% saturation decreases in the order of $\rho^- > \rho^0 > \rho^+$.[58]

Figure 4C shows the semilogarithmic plots of the binding capacity B_X for receptors with different cooperativity parameters. The value of the binding capacity at half-saturation describes the effect of cooperativity interactions between the binding sites. The exact value of the binding capacity for a system with two binding sites can be obtained by substituting the concentration of free ligand at $\bar{N}_X$ = 1.0 (i.e., $[X]^{50\%} = \beta_2^{-1/2}$) in the expression for the binding capacity (eq 8), which gives

$$B_X = \frac{1}{1 + (1/\rho)^{1/2}} \tag{32}$$

Thus, a receptor with two equivalent sites (ρ = 1) has a maximum binding capacity of B_X = 0.5. Similarly, we calculate a maximum value of B_X = 5/6 for a receptor with ρ = 25. In addition, the limiting value of B_X in a receptor with infinite positive cooperativity ($\rho \to \infty$) is 1.0. In the case of a receptor with negative cooperativity (ρ = 1/25), the binding capacity at half-saturation corresponds to a minimum value. However, B_X has two maxima at half-saturations of the first and second binding sites, respectively (i.e., $\bar{N}_X$ = 0.5 and 1.5). These maxima are equivalent to the maximum value of B_X for a receptor with one binding site (Figure 1C). Thus, a receptor with negative cooperativity is mathematically equivalent to a receptor with two independent binding sites.[40]

5.3. Theoretical Evaluation of $\bar{N}_X$ and $d\bar{N}_X/d\Phi$ in a Titration Experiment. Using the dimensionless mass-balance expression in eq 13, we derive an expression to evaluate the extent of titration Φ as a function of $\bar{N}_X$ for the titration of a receptor with *two* binding sites. The mass-balance equation for a receptor with *n* = 2 and cooperative binding interactions is

$$\Phi = \bar{N}_X + \frac{c_\rho}{c_{1/2}} \tag{33}$$

where $c_{1/2}$ corresponds to the ratio between the total receptor concentration and the free ligand concentration at half-

dx.doi.org/10.1021/jp311812a | J. Phys. Chem. B 2013, 117, 8659−8672

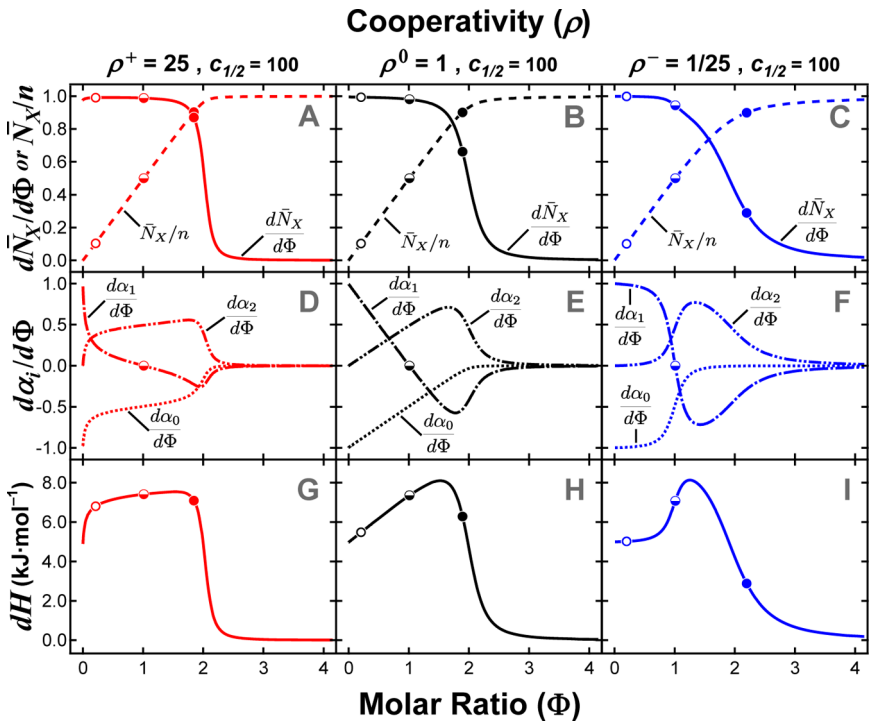

Figure 5. Effects of cooperativity on the binding curves for a receptor with two binding sites (n = 2). The columns represent positive cooperativity, noncooperativity, and negative cooperativity parameters for the binding curves. The 10, 50, and 90% saturation points are indicated, respectively, by open (○), half-filled (◒), and filled circles (●). (A–C) Titration representation of $\bar{N}_X/n$ and $d\bar{N}_X/d\Phi$ vs the extent of titration (Φ). (D–F) Differential change in the mole fractions of the binding species with respect to the mole equivalents of titrant added. The differential change in the mole fraction of the binding species [M] (α_0), [MX] (α_1), and [MX$_2$] (α_2) are represented by the dotted, dash-dotted, and dash-double-dotted lines, respectively. (G–I) Simulated curves of the mole-normalized differential heat for a titration (dH) vs the extent of titration (Φ).

saturation (i.e., $M_T/[X]^{50\%} = M_T \cdot \beta_2^{1/2}$) and c_ρ is a dimensionless variable that depends on the cooperativity parameter ρ and the average ligand binding saturation $\bar{N}_X$ (see the Supporting Information, eq 83). The term $c_{1/2}$ in eq 33 is similar to the c parameter from the WI model (eq 1). Thus, titration experiments with $c_{1/2} \geq 10$ give differential binding curves with an overall sigmoidal shape.

The extent of titration (Φ) to saturate 90% of the binding sites (i.e., $\bar{N}_X = 20/11$) is calculated with the expressions

$$\Phi^{90\%} = \frac{20}{11} + \frac{c_\rho^{90\%}}{c_{1/2}} \tag{34a}$$

$$c_\rho^{90\%} = \frac{1}{\rho^{1/2}} \cdot \left(\frac{9}{2} + \left(\left(\frac{9}{2} \right)^2 + 10\rho \right)^{1/2} \right) \tag{34b}$$

Here $c_\rho^{90\%}$ corresponds to the product of $\beta_2^{1/2}[X]^{90\%}$, as calculated from eq 31. The stepwise binding parameter ρ in eq 34b can also be expressed as a ratio of cumulative binding constants (β_i), or the stepwise binding constants (K_i) using the definitions in eq 30 and in Table 1. We present additional expressions to evaluate the dimensionless cooperativity variable and the degree of titration at 10 and 50% receptor saturation in the Supporting Information (eqs S84 and S85).

Figure 5 shows the effect of positive, negative, or noncooperative interactions on the integral and differential binding curves of a receptor with two binding sites. We simulated the binding curves using a value of $c_{1/2}$ = 100 with all three cooperativity scenarios. Similarly, we modeled the differential heat per mole curves (dH) using the same enthalpy parameters of ΔH_1 = 5.0 kJ·mol^{-1} and ΔH_2 = 15.0 kJ·mol^{-1} in all three cooperativity scenarios, where ΔH_1 and ΔH_2 correspond to the first and second cumulative enthalpies, respectively. The integral and differential curves for the fractional saturation $\bar{N}_X/n$ are shown in Figure 5A–C. By modeling titration experiments with a strong $c_{1/2}$ parameter, we obtain binding curves for $\bar{N}_X/n$ with a hyperbolic shape in the titration range from 0 to 4 equiv. The initial values for the differentials $d\bar{N}_X/d\Phi$ are approximately 1.0. In addition, we observe saturation levels of $\bar{N}_X$ = 1.0 after 1 equiv of ligand is added and $\bar{N}_X$ = 20/11 after approximately 2 equiv of ligand are injected. Positive cooperativity increases the overall stability of the bound species. As a result, both the saturation and the differential binding curves are more rectangular than in the noncooperativity case. The effect of cooperativity is more evident in receptors with negative cooperativity interactions (Figure 5C). In this case, more than 2 equiv of ligand are required to reach the thermodynamic end-point of the titration, and the differential binding curve has a longer sigmoidal transition than in the noncooperative case.

The dimensionless cooperativity variable is c_ρ = 9 for receptors with two sites and noncooperative interactions. Thus, we obtain an expression for $\Phi^{90\%}$ in eq 34a similar to a binding system with n-equivalent binding sites (eq 36). In the case of positive cooperativity (ρ = 25), the dimensionless cooperativity variable is $c_\rho \approx 4.2$. This means that the concentration of free ligand at equilibrium is lower than that for ρ = 1 and that a shorter titration range is required to reach 90% saturation. In contrast, receptors with negative cooperativity interactions require a higher extent of titration to reach 90% saturation. For example, a receptor with a cooperativity parameter of ρ = 1/25

dx.doi.org/10.1021/jp311812a | J. Phys. Chem. B 2013, 117, 8659–8672

has a cooperativity titration coefficient of $c_\rho \approx 45$. Thus, the concentration of free ligand is approximately 5 times larger than that for $\rho = 1$, and a larger titration range is required.

The effect of the cooperativity parameter ρ on the differential binding curves can be observed in more detail by decomposing the differential binding curve $d\bar{N}_X/d\Phi$ into its mole fraction components $d\alpha_i/d\Phi$, as shown in Figure 5D–F. In fact, differential binding curves that appear symmetrical at first (Figure 5A,B) have more interesting features when evaluated in terms of $d\alpha_i/d\Phi$. In Figure 5D, for example, we observe a sharp decrease in the differential mole fraction for the singly bound state ($d\alpha_1/d\Phi$) and a corresponding increase for the differential mole fraction for the doubly bound state ($d\alpha_2/d\Phi$) for a receptor with positive cooperativity. For receptors with equivalent binding sites ($\rho^0 = 1$), there is a steady decrease in the contribution of $d\alpha_1/d\Phi$ and a steady increase in the contribution of $d\alpha_2/d\Phi$, where $d\alpha_2/d\Phi$ cancels the effect of $d\alpha_1/d\Phi$ after the differentials are adjusted by their respective stoichiometry coefficients (i.e., $2\cdot d\alpha_2/d\Phi$ in eq 28). Finally, in receptors with a negative cooperativity parameter of $\rho^- = 1/25$, we observe a sigmoidal transition from the singly bound state to the doubly bound state, consistent with expectations for a sequential binding site model.

In addition to using $d\alpha_i/d\Phi$ to decompose the differential binding curve, we can use the differential change in the receptor mole fractions to model the differential heat per mole titration curves (dH). In the limit of $\Phi \rightarrow 0$, the dH curves are approximately equal to ΔH_1 (i.e., 5.0 kJ·mol^{-1}) in the three cooperativity scenarios. The dH curves have maxima of approximately 8.0 kJ·mol^{-1} at $\Phi = 1.5$, as given by the expression $dH_{\Phi=1.5} \approx (\Delta H_2 - \Delta H_1)\cdot d\alpha_2/d\Phi$. The differential heat curves have different transition profiles from the initial values to the maxima. For example, the differential dH curve of a receptor with positive cooperativity has a hyperbolic shape in the range from $\Phi = 0.0$ to 1.5. As a result, the initial injection points hold important information about the enthalpy of binding ΔH_1 as well as the cooperativity parameter ρ. The differentials dH for receptors with noncooperativity have a linear shape, while those with negative cooperativity have a sigmoidal transition over the titration range from $\Phi = 0.0$ to 1.5. The linear transition in a receptor with *two* equivalent binding sites is not commonly observed because receptors with two equivalent sites also have equivalent enthalpies of binding for each site. As a result, the cumulative enthalpies account for the stoichiometry of the bound state such that $\Delta H_2 = 2\Delta H_1$ (see Table 1), and the dH curve has a symmetric shape that resembles $d\bar{N}_X/d\Phi$ in Figure 5B. The dH curve presented for $\rho = 1$ resembles a receptor with two independent binding sites of nearly equivalent binding strength (i.e., $k_{11} \approx k_{21}$) but different enthalpies of binding. The profile of dH in a receptor with negative cooperativity is typically observed in stepwise binding processes.

Detecting or confirming positive cooperativity experimentally can be challenging. In most ITC experiments, the first injection point is discarded due to passive diffusion of the ligand from the tip of the syringe to the titration cell as well as the "backlash effect".[59] Therefore, when assessing a receptor with possible positive cooperativity, it is important to evaluate the heat at the initial injection points. To obtain better estimates of the enthalpy and cooperativity parameters, the number of injections must be increased in the Φ range 0.0–0.5. Alternatively, the initial receptor concentration can be decreased to decrease the magnitude of $c_{1/2}$ and to evaluate the titration over a longer titration range.

5.4. Experimental Evaluation of the Gd-Citrate Titration with a DBM. The ITC experiment for the titration of Gd(III) with citrate ligand is shown in Figure 6. The thermogram obtained after subtracting the noise-filtered baseline shown in the upper panel of Figure 6A, whereas the thermogram prior to baseline correction is shown in the bottom panel. The interaction between gadolinium and citrate ligand (Cit) has two distinct heats of reaction, as shown by the exothermic peaks before 90 min that correspond to the 1:1 complex, and the highly exothermic peaks after 90 min that correspond to the 1:2 complex. The differential heat per mole

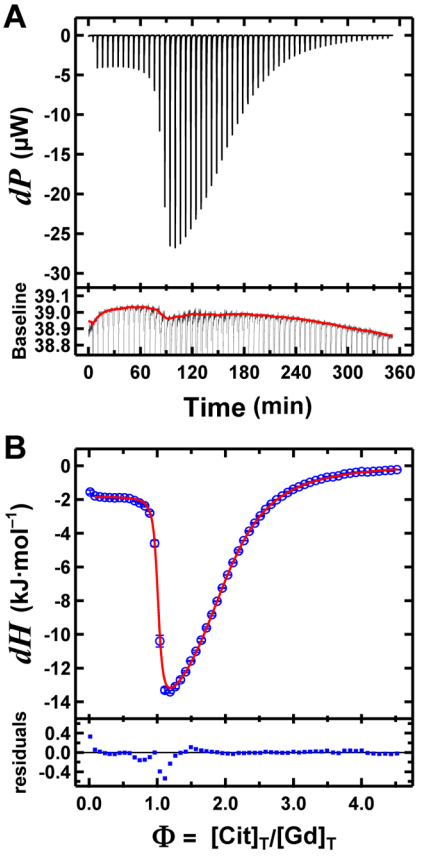

Figure 6. Isothermal titration calorimetry of Gd(III) with sodium citrate in MES buffer (100 mM, pH 5.5). (A) Baseline-corrected thermogram for one of the replicates in the titration calorimetry experiment. The exothermic peaks before $t = 90$ min correspond to the formation of the 1:1 Gd–citrate complex, while the peaks after $t = 90$ min correspond to the 1:2 complex. An expanded view of the raw thermogram in the bottom panel shows the corrected baseline after smoothing the original baseline with the Savitzky–Golay noise filter. (B) Averaged values of the differential heat per mole from three replicates. The error bars in the titration curve indicate the standard deviation (σ_k) from the averaged $d\bar{H}_k$ values, and the line indicates the fitting curve. The residuals for the weighted nonlinear least-squares regression analysis are shown in the bottom panel of part B. Only small deviations between the model and the experimental data are present at a degree of titration near $\Phi = 1.0$, which gives a reduced chi-square value of $\chi_\nu^2 = 1.92$. Thus, the DBM for a receptor with $n = 2$ is in good agreement with the experimental data. For comparison, we include the titration curves analyzed with the *sequential-sites* and the *two-sites* models included with the analysis software of the calorimeter (Origin 7.0) in the Supporting Information (Figure S5).

dx.doi.org/10.1021/jp311812a | J. Phys. Chem. B 2013, 117, 8659–8672

Table 2. Thermodynamic and Statistical Parameters for the Titration of Gd(III) with Sodium Citrate in MES Buffer (100 mM, pH 5.5)[a]

	DBM		Origin							
binding parameters	best fit value	+/−	best fit value	+/−	correlation matrix					
N	1.01	0.001			1	0.24	0.53	−0.13	0.90	−0.26
log K_1	7.07	0.03	7.18	0.07		1	0.15	−0.38	0.28	−0.13
log K_2	4.13	0.004	4.13	0.003			1	−0.05	0.76	−0.78
ΔH_1^0 (kJ·mol^{-1})	−1.84	0.01	−2.06	0.01				1	−0.13	0.04
ΔH_2^1 (kJ·mol^{-1})	−16.57	0.06	−16.68	0.02					1	−0.58
Δh_{dil} (kJ·mol^{-1})	0.19	0.01	0.21[b]							1
χ_ν^2	1.92[c]		5.45							

[a]For comparison, we provide the binding parameters obtained using the sequential sites binding model in Origin 7.0. [b]In Origin, the heat of dilution was adjusted manually by adding or subtracting small heat values (ca. 0.02 kJ·mol^{-1}) until we obtained a minimum value for χ_ν^2. [c]The reduced chi-square value (χ_ν^2) of the DBM model for a sequential binding site interaction shows considerable improvement in comparison with the model provided with the analysis software for the calorimeter (Origin 7.0). Our DBM includes two additional binding parameters that correspond to an stoichiometry coefficient that adjusts the concentration of the receptor (i.e., $M_T^* = N{\cdot}M_T$) and an enthalpy of dilution (Δh_{dil}).

(dH) signal for the Gd(III)−Cit titration is shown in the upper panel of Figure 6B. The initial (ca. −2.0 kJ·mol^{-1}) and minimum (ca. −14.0 kJ·mol^{-1}) values in the dH vs Φ titration plot may be used as guess values for the enthalpies of binding of the 1:1 and 1:2 Gd(III)−Cit complexes during the fitting process. The line in Figure 6B represents the fitted curve obtained from the weighted nonlinear regression analysis using a DBM with $n = 2$. Commonly, the binding parameters for the complexation of metal ions with small ligands are obtained using a model constrained for sequential binding sites.[48] Thus, we use a DBM constrained for sequential binding sites to analyze the Gd(III)−Cit calorimetry titration.

The results of the nonlinear regression analysis with the DBM are summarized in Table 2. For comparison, we include the results obtained using the sequential sites binding model included with the analysis software of the calorimeter (embedded in Origin 7.0). The averaged heat per mole data in Origin was also weighted by σ_k^{-1} (eq 18) during the nonlinear regression analysis. There is good agreement between the binding parameters obtained with the two fitting algorithms. Thus, the DBM is equivalent to the built-in model in Origin constrained to represent a receptor with two sequential sites. The algorithm in the built-in software, however, does not allow the end user to correct the titration curve for small experimental errors in the concentration of receptor (e.g., $M_T^* = N{\cdot}M_T$) or to automatically adjust for the heat of dilution (Δh_{dil}). By including these fitting parameters in our DBM, we obtain a smaller χ_ν^2 value in comparison to the sequential binding sites model in Origin (χ_ν^2(DBM) = 1.92 vs χ_ν^2(Origin) = 5.45).

Binding models with a higher number of fitting parameters are expected to have lower χ_ν^2 values due to the increased flexibility of the fitting curve. We can use the F-test[53] to determine whether the additional binding parameters are valid from a statistical perspective, which gives $F_\chi = 96.5$ with a critical value of $F_{Crit} = 4.03$ for each additional binding parameter. Since $F_\chi > F_{Crit}$, the additional binding parameters in the DBM are statistically valid. For comparison, we show the fitting curve obtained with the sequential binding sites algorithm in Origin (Supporting Information, Figure S5A).

The titration curve in Figure 6B resembles the simulated dH curve of a receptor with negative cooperativity (Figure 5I). Thus, DBMs constrained to represent receptors with cooperative or independent interactions can also be applied to the experimental data. First, we show the binding parameters obtained with the general and cooperative DBMs (Supporting Information, Table S1). We obtained the same fitting curve and the same value of $\chi_\nu^2 = 1.92$ for all the DBMs studied. This result confirms that all the DBMs are mathematically equivalent in a receptor with $2(\beta_2)^{1/2} < \beta_1$ (eq 30). Then, we compared the thermodynamic parameters obtained with the DBM constrained for receptors with two independent binding sites and the *two-sites* model in Origin (Table S2 and Figure S5B, Supporting Information). The thermodynamic parameters obtained with the algorithms that account for two independent sites are in good agreement with reduced chi-square parameters of $\chi_\nu^2 = 1.92$ for the DBM and $\chi_\nu^2 = 1.96$ for the algorithm in Origin. We expected a lower χ_ν^2 value with the algorithm in Origin because it contains two stoichiometry parameters (N_1, N_2). However, the χ_ν^2 values from the DBM and from Origin are equivalent, which suggests that the additional stoichiometry parameter is not valid. This agrees with the physical model where a central metal ion is able to coordinate with two ligand species, and thus it must have the same stoichiometry value for the first site as it has for the second site.

The correlation matrix in Table 2 shows the dependency among the fitting parameters in the DBM. Correlation values close to 1.0 or −1.0 in the matrix indicate a strong correlation between the fitting parameters. For example, the stoichiometry coefficient N that adjusts the concentration of receptor in the titration cell is strongly correlated to the stepwise enthalpy of binding ΔH_2^1 (Corr(N, ΔH_2^1) = 0.90). The stoichiometry coefficient N shifts the location of the inflection point around $\Phi = 1.0$ and stretches the fitting curve horizontally. Thus, an increase in the value of N would require a comparable increase in the value ΔH_2^1 in order to fit the points near $\Phi = 1.0$.

The thermodynamic parameters for the complexation of Gd(III) with citrate ligand can be refined further to account for the effect of pH on the binding equilibrium as well as the protons exchanged with the buffer during the complexation. We plan to present the DBMs that account for the effect of the protons and the buffer in a future publication.

6. RECEPTOR WITH MULTIPLE BINDING SITES: INDEPENDENT AND EQUIVALENT MODELS

The DBM in eqs 14a−14c can be extended to account for a receptor with n-independent binding sites. The differential change in the mole fraction of the ith bound site is given by

dx.doi.org/10.1021/jp311812a | J. Phys. Chem. B 2013, 117, 8659−8672

$$dH = \sum_{i=1}^{n} \left(\Delta h_{i1} \frac{d\alpha_{i1}}{d\Phi} \right) \tag{35a}$$

$$\frac{d\alpha_{i1}}{d\Phi} = \frac{c_{(i)}}{c_{(i)} + (P_{M(i)})^2 (1 + \sum_{j=1, j\neq i}^{n} (c_{(j)}/(P_{M(j)})^2))} \tag{35b}$$

where the dimensionless binding parameter for the ith site is given by $c_{(i)} = M_T \cdot k_{i1}$ and the corresponding binding polynomial is given by $P_{M(i)} = 1 + k_{i1}[X]$. Furthermore, this model can be extended to account for a receptor with n equivalent binding sites, as given by

$$dH = \Delta h \cdot \frac{n c_{eq}}{n c_{eq} + (P_M)^2} \tag{36}$$

where c_{eq} corresponds to the product of the intrinsic binding constant k and the total receptor concentration (i.e., $c_{eq} = M_T \cdot k$). In eq 36, the number n of binding sites is a natural number and should not be confused with the active fraction of binding species (f_a)[12] or N which are rational numbers. Commonly, the parameters f_a or N account for small errors in the total concentration of either the receptor or ligand species.

7. CONCLUSIONS

We have developed a general form of the differential binding model (DBM) for ITC experiments that can be applied to receptors with multiple binding sites in which the interactions among the binding sites are not constrained to a specific binding mechanism. This demonstrates that equations such as the Wiseman isotherm can be generalized with a DBM derived from the binding polynomial. We have confirmed this by obtaining titration curves equivalent to those obtained using the models by Wiseman and others.[20,40] In addition, we have shown the applicability of the general binding model to represent receptors with specific binding interactions among the binding sites, such as in the case of a receptor with *two* binding sites and cooperative binding interactions as well as two sites and sequential binding sites, as shown for the titration between Gd(III) and citrate ligand. Similarly, we developed a DBM for a receptor with independent binding sites, each with a distinct binding affinity. We expect that these equations will aid in the selection of binding models for the analysis of ITC experiments.

■ ASSOCIATED CONTENT

Supporting Information

We include a step-by-step derivation of the general DBM for a receptor with multiple binding sites and a detailed evaluation of the general DBM for receptors with either one or two binding sites (n = 1, 2). In the case of a receptor with n = 2, we show how the general DBM can be used to represent different binding interactions between the sites. We also show additional analyses of the titration of Gd(III) with citrate ligand using the built-in models included in Origin 7.0. This material is available free of charge via the Internet at http://pubs.acs.org.

■ AUTHOR INFORMATION

Corresponding Author

*E-mail: mwinnik@chem.utoronto.ca.

Notes

The authors declare no competing financial interest.

■ ACKNOWLEDGMENTS

The authors thank NSERC Canada and the Province of Ontario for their support of this research. We also would like to thank Dr. G. Guerin and Professor H. Heerklotz for their valuable comments and discussions about this manuscript.

■ REFERENCES

(1) Wiseman, T.; Williston, S.; Brandts, J. F.; Lin, L.-N. Rapid Measurement of Binding Constants and Heats of Binding Using a New Titration Calorimeter. *Anal. Chem.* **1989**, *179*, 131−137.

(2) Freire, E.; Mayorga, O. L.; Straume, M. Isothermal Titration Calorimetry. *Anal. Chem.* **1990**, *62*, 950A−959A.

(3) Cooper, A. Microcalorimetry of Protein-Protein Interactions. In *Protein Targeting Protocols*; Clegg, R. A., Walker, J. M., Eds.; Methods in Molecular Biology; Humana Press: Totowa, NJ, 1998; Vol. *88*, pp 11−22.

(4) Mandal, D. K.; Kishore, N.; Brewer, C. F. Thermodynamics of Lectin-Carbohydrate Interactions. Titration Microcalorimetry Measurements of the Binding of *N*-Linked Carbohydrates and Ovalbumin to Concanavalin A. *Biochemistry* **1994**, *33*, 1149−1156.

(5) Buurma, N. J.; Haq, I. Advances in the Analysis of Isothermal Titration Calorimetry Data for Ligand-DNA Interactions. *Methods* **2007**, *42*, 162−172.

(6) Bouchemal, K.; Agnely, F.; Koffi, A.; Djabourov, M.; Ponchel, G. What Can Isothermal Titration Microcalorimetry Experiments Tell Us About the Self-Organization of Surfactants into Micelles? *J. Mol. Recognit.* **2009**, *23*, 335−342.

(7) Bjelić, S.; Jelesarov, I. A Survey of the Year 2007 Literature on Applications of Isothermal Titration Calorimetry. *J. Mol. Recognit.* **2008**, *21*, 289−312.

(8) Falconer, R. J.; Collins, B. M. Survey of the Year 2009: Applications of Isothermal Titration Calorimetry. *J. Mol. Recognit.* **2011**, *24*, 1−16.

(9) Ghai, R.; Falconer, R. J.; Collins, B. M. Applications of Isothermal Titration Calorimetry in Pure and Applied Research-Survey of the Literature from 2010. *J. Mol. Recognit.* **2012**, *25*, 32−52.

(10) Majonis, D.; Herrera, I.; Ornatsky, O.; Schulze, M.; Lou, X.; Soleimani, M.; Nitz, M.; Winnik, M. A. Synthesis of a Functional Metal-Chelating Polymer and Steps toward Quantitative Mass Cytometry Bioassays. *Anal. Chem.* **2010**, *82*, 8961−8969.

(11) Gans, P.; Sabatini, A.; Vacca, A. Simultaneous Calculation of Equilibrium Constants and Standard Formation Enthalpies from Calorimetric Data for Systems with Multiple Equilibria in Solution. *J. Solution Chem.* **2008**, *37*, 467−476.

(12) Houtman, J. C. D.; Brown, P. H.; Bowden, B.; Yamaguchi, H.; Appella, E.; Samelson, L. E.; Schuck, P. Studying Multisite Binary and Ternary Protein Interactions by Global Analysis of Isothermal Titration Calorimetry Data in SEDPHAT: Application to Adaptor Protein Complexes in Cell Signaling. *Protein Sci.* **2007**, *16*, 30−42.

(13) Buurma, N. J.; Haq, I. Calorimetric and Spectroscopic Studies of Hoechst 33258: Self-Association and Binding to Non-Cognate DNA. *J. Mol. Biol.* **2008**, *381*, 607−621.

(14) Krishnamoorthy, J.; Mohanty, S. Open-ITC: An Alternate Computational Approach to Analyze the Isothermal Titration Calorimetry Data of Complex Binding Mechanisms. *J. Mol. Recognit.* **2011**, *24*, 1056−1066.

(15) Brocos, P.; Banquy, X.; Díaz-Vergara, N.; Pérez-Casas, S.; Piñeiro, Á.; Costas, M. A Critical Approach to the Thermodynamic Characterization of Inclusion Complexes: Multiple-Temperature Isothermal Titration Calorimetric Studies of Native Cyclodextrins with Sodium Dodecyl Sulfate. *J. Phys. Chem. B* **2011**, *115*, 14381−14396.

(16) Le, V. H.; Buscaglia, R.; Chaires, J. B.; Lewis, E. A. Modeling Complex Equilibria in Isothermal Titration Calorimetry Experiments: Thermodynamic Parameters Estimation for a Three-Binding-Site Model. *Anal. Biochem.* **2013**, *434*, 233−241.

(17) Velazquez-Campoy, A.; Goñi, G.; Peregrina, J. R.; Medina, M. Exact Analysis of Heterotropic Interactions in Proteins: Character-

ization of Cooperative Ligand Binding by Isothermal Titration Calorimetry. *Biophys. J.* **2006**, *91*, 1887−1904.
(18) Velazquez-Campoy, A.; Freire, E. Isothermal Titration Calorimetry to Determine Association Constants for High-Affinity Ligands. *Nat. Protoc.* **2006**, *1*, 186−191.
(19) Iversen, R.; Andersen, P. A.; Jensen, K. S.; Winther, J. R.; Sigurskjold, B. W. Thiol−Disulfide Exchange between Glutaredoxin and Glutathione. *Biochemistry* **2010**, *49*, 810−820.
(20) Poon, G. M. K. Explicit Formulation of Titration Models for Isothermal Titration Calorimetry. *Anal. Biochem.* **2010**, *400*, 229−236.
(21) Asuero, A. G.; Michałowski, T. Comprehensive Formulation of Titration Curves for Complex Acid-Base Systems and Its Analytical Implications. *Crit. Rev. Anal. Chem.* **2011**, *41*, 151−187.
(22) Tyrrel, H. J. V. End-Point Sharpness in Thermometric Titrimetry. *Talanta* **1967**, *14*, 843−848.
(23) Momoki, K.; Sekino, J.; Sato, H.; Yamaguchi, N. Theory of Curved Molar Ratio Plots and a New Linear Plotting Method. *Anal. Chem.* **1969**, *41*, 1286−1299.
(24) Tellinghuisen, J. Optimizing Experimental Parameters in Isothermal Titration Calorimetry. *J. Phys. Chem. B* **2005**, *109*, 20027−20035.
(25) Tellinghuisen, J. A Study of Statistical Error in Isothermal Titration Calorimetry. *Anal. Biochem.* **2003**, *321*, 79−88.
(26) Turnbull, W. B.; Daranas, A. H. On the Value of *c*: Can Low Affinity Systems Be Studied by Isothermal Titration Calorimetry? *J. Am. Chem. Soc.* **2003**, *125*, 14859−14866.
(27) Hansen, L. D.; Fellingham, G. W.; Russell, D. J. Simultaneous Determination of Equilibrium Constants and Enthalpy Changes by Titration Calorimetry: Methods, Instruments, and Uncertainties. *Anal. Biochem.* **2011**, *409*, 220−229.
(28) Broecker, J.; Vargas, C.; Keller, S. Revisiting the Optimal *c* Value for Isothermal Titration Calorimetry. *Anal. Biochem.* **2011**, *418*, 307−309.
(29) Indyk, L.; Fisher, H. F. Theoretical Aspects of Isothermal Titration Calorimetry. In *Energetics of Biological Macromolecules Part B*; Ackers, G. K., Johnson, M. L., Eds.; Methods in Enzymology; Academic Press: San Diego, CA, 1998; Vol. *295*, pp 350−364.
(30) Markova, N.; Hallén, D. The Development of a Continuous Isothermal Titration Calorimetric Method for Equilibrium Studies. *Anal. Biochem.* **2004**, *331*, 77−88.
(31) Wyman, J.; Gill, S. J. *Binding and Linkage: Functional Chemistry of Biological Macromolecules*; University Science Books: Mill Valley, CA, 1990.
(32) Wyman, J. The Binding Potential, a Neglected Linkage Concept. *J. Mol. Biol.* **1965**, *11*, 631−644.
(33) Alberty, R. A. Thermodynamics of the Binding of Ligands by Macromolecules. *Biophys. Chem.* **1996**, *62*, 141−159.
(34) Poland, D. Protein-Binding Polynomials. *J. Protein Chem.* **2001**, *20*, 91−97.
(35) Johnson, M. L.; Straume, M. Deriving Complex Ligand-Binding Formulas. In *Energetics of Biological Macromolecules, Part C*; Johnson, M. L., Ackers, G. K., Eds.; Methods in Enzymology; Academic Press: San Diego, CA, 2000; Vol. *323*, pp 155−167.
(36) Onufriev, A.; Ullmann, G. M. Decomposing Complex Cooperative Ligand Binding into Simple Components: Connections between Microscopic and Macroscopic Models. *J. Phys. Chem. B* **2004**, *108*, 11157−11169.
(37) Gill, S. J.; Richey, B.; Bishop, G.; Wyman, J. Generalized Binding Phenomena in an Allosteric Macromolecule. *Biophys. Chem.* **1985**, *21*, 1−14.
(38) Castronuovo, G.; Elia, V.; Fessas, D.; Velleca, F.; Viscardi, G. Thermodynamics of the Interaction of α-Cyclodextrin with Monocarboxylic Acids in Aqueous Solutions: A Calorimetric Study at 25 °C. *Carbohydr. Res.* **1996**, *287*, 127−138.
(39) El Harrous, M.; Parody-Morreale, A. Measurement of Biochemical Affinities with a Gill Titration Calorimeter. *Anal. Biochem.* **1997**, *254*, 96−108.
(40) Freire, E.; Schön, A.; Velazquez-Campoy, A. Isothermal Titration Calorimetry: General Formalism Using Binding Polynomials. In *Biothermodynamics, Part A*; Johnson, M. L., Holt, J. M., Ackers, G. K., Eds.; Methods in Enzymology; Academic Press: San Diego, CA, 2009; Vol. *455*, pp 127−155.
(41) Koper, G. J. M.; Minkenberg, C. B.; Upton, I. S.; van Esch, J. H.; Sudhölter, E. J. R. Quantitatively Interpreting Thermal Behavior of Self-Associating Systems. *J. Phys. Chem. B* **2009**, *113*, 15597−15601.
(42) Di Cera, E.; Chen, Z. Q. The Binding Capacity Is a Probability Density Function. *Biophys. J.* **1993**, *65*, 164−170.
(43) Grolier, J.-P. E.; Del Río, J. M. Isothermal Titration Calorimetry: A Thermodynamic Interpretation of Measurements. *J. Chem. Thermodyn.* **2012**, *55*, 193−202.
(44) Blandamer, M. J.; Cullis, P. M.; Engberts, J. B. F. N. Titration Microcalorimetry. *Faraday Trans.* **1998**, *94*, 2261−2267.
(45) Zhu, M. M.; Rempel, D. L.; Du, Z.; Gross, M. L. Quantification of Protein−Ligand Interactions by Mass Spectrometry, Titration, and H/D Exchange: PLIMSTEX. *J. Am. Chem. Soc.* **2003**, *125*, 5252−5253.
(46) Vinnakota, K.; Kemp, M. L.; Kushmerick, M. J. Dynamics of Muscle Glycogenolysis Modeled with pH Time Course Computation and pH-Dependent Reaction Equilibria and Enzyme Kinetics. *Biophys. J.* **2006**, *91*, 1264−1287.
(47) Lapitsky, Y.; Parikh, M.; Kaler, E. W. Calorimetric Determination of Surfactant/Polyelectrolyte Binding Isotherms. *J. Phys. Chem. B* **2007**, *111*, 8379−8387.
(48) Smith, R. M.; Martell, A. E.; Motekaitis, R. J. NIST Standard reference database 46. *NIST Critically Selected Stability Constants of Metal Complexes Database Ver 8.0*, 2004.
(49) Henzl, M. T. Characterization of Parvalbumin and Polcalcin Divalent Ion Binding by Isothermal Titration Calorimetry. In *Biothermodynamics, Part A*; Johnson, M. L., Holt, J. M., Ackers, G. K., Eds.; Methods in Enzymology; Academic Press: San Diego, CA, 2009; Vol. *455*, pp 259−297.
(50) Keller, S.; Vargas, C.; Zhao, H.; Piszczek, G.; Brautigam, C. A.; Schuck, P. High-Precision Isothermal Titration Calorimetry with Automated Peak-Shape Analysis. *Anal. Chem.* **2012**, *84*, 5066−5073.
(51) Sigurskjold, B. W. Exact Analysis of Competition Ligand Binding by Displacement Isothermal Titration Calorimetry. *Anal. Biochem.* **2000**, *277*, 260−266.
(52) Jenkins, M. A. Algorithm 493: Zeros of a Real Polynomial [C2]. *ACM Trans. Math. Software* **1975**, *1*, 178−189.
(53) Bevington, P. R. *Data Reduction and Error Analysis for the Physical Sciences*, 3rd ed.; McGraw-Hill: Boston, MA, 2003.
(54) Zwolak, J. W.; Boggs, P. T.; Watson, L. T. Algorithm 869: ODRPACK95: A Weighted Orthogonal Distance Regression Code with Bound Constraints. *ACM Trans. Math. Software* **2007**, *33*, 27.
(55) Heerklotz, H.; Lantzsch, G.; Binder, H.; Klose, G.; Blume, A. Thermodynamic Characterization of Dilute Aqueous Lipid/Detergent Mixtures of POPC and $C_{12}EO_8$ by Means of Isothermal Titration Calorimetry. *J. Phys. Chem.* **1996**, *100*, 6764−6774.
(56) Douglass, E. F.; Miller, C. J.; Sparer, G.; Shapiro, H.; Spiegel, D. A. A Comprehensive Mathematical Model for Three-Body Binding Equilibria. *J. Am. Chem. Soc.* **2013**, *135*, 6092−6099.
(57) Sackett, D. L.; Saroff, H. A. The Multiple Origins of Cooperativity in Binding to Multi-Site Lattices. *FEBS Lett.* **1996**, *397*, 1−6.
(58) Hunter, C. A.; Anderson, H. L. What is Cooperativity? *Angew. Chem., Int. Ed.* **2009**, *48*, 7488−7499.
(59) Mizoue, L. S.; Tellinghuisen, J. The Role of Backlash in the "First Injection Anomaly" in Isothermal Titration Calorimetry. *Anal. Biochem.* **2004**, *326*, 125−127.